Kidney International, Vol. 66 (2004), pp. 1815–1825

CELL BIOLOGY – IMMUNOLOGY – PATHOLOGY

The renin-angiotensin system blockade does not prevent renal interstitial fibrosis induced by aristolochic acids

FRÉDÉRIC D. DEBELLE, JOËLLE L. NORTIER, CÉCILE P. HUSSON, ERIC G. DE PREZ, ANNE R. VIENNE, KATJA ROMBAUT, ISABELLE J. SALMON, MONIQUE M. DESCHODT-LANCKMAN, and JEAN-LOUIS VANHERWEGHEM

Laboratory for Research on Peptide Metabolism, Faculty of Medicine; and Departments of Nephrology and Pathology, Erasme Hospital, Université Libre de Bruxelles, Brussels, Belgium

The renin-angiotensin system blockade does not prevent renal interstitial fibrosis induced by aristolochic acids.

Background. Experimental aristolochic acid nephropathy (AAN), characterized by interstitial fibrosis, tubular atrophy, and chronic renal failure, was reported after 35-day injections of aristolochic acids (AA) to salt-depleted male Wistar rats. The link between renal fibrosis and the renin-angiotensin system (RAS) in this model remains unknown.

Methods. We investigated the impact of sodium diets (low and normal), of RAS inhibition with enalapril (ENA) alone, or combined with candesartan (CSN) for 35 days, and ENA + CSN for 65 days on AAN development. At the end of each observation period, blood pressure and renal angiotensin-converting enzyme activity were measured, as well as renal functional impairment (plasma creatinine increase, proteinuria) and histologic lesions (interstitial fibrosis, monocytes/macrophages infiltration, myofibroblasts collagens type I and IV, proliferating cells).

Results. Sodium intake did not modify renal functional and morphologic impairment induced by AA. The RAS blockade by ENA or ENA + CSN in rats receiving AA did not result in any statistical difference in terms of renal failure, proteinuria, and interstitial fibrosis on day 35 or 65. On day 35, the monocytes/macrophages infiltration was significantly decreased by two-fold when ENA ($P < 0.01$) or ENA + CSN ($P < 0.01$) was given from day 0.

Conclusion. Our data demonstrate that RAS modulation by salt depletion and pharmacologic blockade do not influence renal failure and interstitial fibrosis in the rat model of AAN. We suggest that pathways of interstitial renal fibrosis may be independent of RAS at least in some conditions.

Key words: renin-angiotensin system, angiotensin-converting enzyme inhibitor, angiotensin type 1 receptor antagonist, aristolochic acid, renal fibrosis, rat model, Chinese-herb nephropathy.

Received for publication July 2, 2003
and in revised form April 1, 2004
Accepted for publication May 11, 2004

Irrespective of the underlying cause, chronic renal diseases are characterized by progressive interstitial fibrosis and an increasing loss of renal tubules. It has been largely demonstrated that the renal function decline and long-term prognosis are well correlated with the severity of tubulointerstitial injuries [1, 2]. Regular intake of Chinese medicinal herbs containing nephrotoxic and carcinogenic aristolochic acids (AA) is now recognized as a cause of interstitial renal fibrosis, as well as a risk factor for upper urinary tract carcinoma in humans [3–9]. Taking into account that a first attempt to experimentally reproduce the disease in rodents had failed [10], we successfully developed a rat model of AA nephropathy (AAN) derived from the experimental model of cyclosporine nephropathy [11]. Both models include a salt depletion before the exposure to the nephrotoxic substance [11, 12], leading to the hypothesis that the renin-angiotensin system (RAS) could play an important role in the pathophysiology of renal fibrosis.

Large clinical trials reinforced this hypothesis by demonstrating renoprotective effects of angiotensin-converting enzyme (ACE) inhibitors or angiotensin type 1 receptor antagonists (AT1RA) on the progression of diabetic [13, 14], as well as nondiabetic, renal diseases [15, 16]. Recent short-term studies indicated that AT1RA exhibited antiproteinuric and antihypertensive effects similar to those primarily shown by ACE inhibitors in patients with chronic renal diseases [17, 18]. Moreover, these renoprotective effects seemed to be more pronounced when ACE inhibitors and AT1RA therapy were combined [19]. Experimentally, the RAS blockade with ACE inhibitors or AT1RA was reported to reduce chronic renal lesions in some animal models, such as remnant kidney [20], streptozotocin-induced diabetes mellitus [21, 22], hypertensive renal injury [23], or unilateral ureteral obstruction [24]. This led us to speculate that angiotensin II (Ang II) could play a key role in the fibrotic process of AA-induced nephropathy.

Table 1. Study design

Protocol 1 (35 days)			Protocol 2 (35 days)			Protocol 3 (65 days)		
Rat groups	*N*	Diet	Rat groups	*N*	Diet	Rat groups	*N*	Diet
Control (vehicles)	6	LS	Control (vehicles)	7	NS			
ENA	7	LS	ENA + CSN	7	NS			
AA	7	LS	AA	6	NS	AA for 35 days	6	NS
AA + ENA	7	LS	AA + ENA + CSN	7	NS	AA for 35 days and ENA + CSN for 65 days	6	NS
AA + ENA from day 10	7	LS	AA	7	LS			

Abbreviations are: LS, low sodium; NS, normal sodium; ENA, enalapril (10 mg/kg body wt/day, in drinking water); CSN, candesartan cilexetil (7 mg/kg body wt/day in drinking water); AA, aristolochic acids (10 mg/kg body wt/day, subcutaneous injections for 35 days). Drugs were given from day 0, except when indicated. The rats were sacrificed on day 35 in protocols 1 and 2, and on day 65 in protocol 3.

We therefore investigated the respective roles of salt depletion and ACE inhibitors ± AT1RA on the development of renal fibrosis in rats treated with AA. Starting from the initial model of AAN, which is the daily subcutaneous administration of AA for 35 days, enalapril (ENA) was given either prophylactically (from day 0) or therapeutically (from day 10) to salt-depleted rats intoxicated by AA. Because no beneficial effect was observed [abstract; Debelle FD et al, *J Am Soc Nephrol* 13:344A, 2002], we performed a second protocol addressing two questions: first, whether a low sodium diet was mandatory to enhance the AA-induced renal fibrosis; and second, whether an optimized RAS blockade with a combined therapy ACE inhibitor *plus* AT1RA was beneficial to prevent the progression of this nephropathy. Because no significant prevention by dual RAS blockade was observed after 35 days, we performed a third protocol with a longer period of observation (65 days). Our experimental data showed that stimulation of the RAS did not enhance the renal toxicity of AA, and that the RAS blockade by an ACE inhibitor ± AT1RA did not affect the progression of renal failure and interstitial fibrosis, despite a significant reduction of the macrophage infiltration. Taken together, these data suggest that some pathways leading to interstitial renal fibrosis, such as the pathways involved in AA-induced nephropathy, may be RAS independent.

METHODS

Experimental design

Male Wistar rats (Elevage Janvier, Le Genest Saint-Isle, France) weighing 160 to 210 g (age, 5 to 6 weeks) were housed in a temperature-, humidity-, and light-controlled environment with free access to water and food. Animal care and treatment were approved by the Ethical Committee for Animal Care (Faculty of Medicine, Université Libre de Bruxelles). A mixture of AA, containing 40% aristolochic acid I (AAI) and 60% aristolochic acid II (AAII), was purchased from Acros Organics (Geel, Belgium) and dissolved in polyethylene glycol (PEG) 400 (Fluka Chemie, Buchs, Switzerland) to a final concentration of 20 mg/mL, and diluted in distilled water before subcutaneous injection at a dose of 10 mg/kg body weight. The ACE inhibitor enalapril (ENA; Sigma Aldrich, Bornem, Belgium) and the AT1RA candesartan cilexetil (CSN; a gift from Astra Zeneca Research laboratories, Mölndal, Sweden) were prepared as a stock solution of 200 mg/L and 100 mg/L, respectively, and administrated in the drinking water at the daily dosage of 10 mg/kg body weight for enalapril, and 7 mg/kg body weight for candesartan. Due to its poor solubility in water, CSN was first solubilized in vehicle comprising PEG400 (0.1% vol/vol), sodium bicarbonate (5 mmol/L), and ethanol (0.1% vol/vol). Drinking consumption and body weight were recorded three times a week for drug dosage adjustment.

In the first protocol (Table 1), 34 salt-depleted rats were randomly divided into five groups and submitted to the following treatments for a 35-day period: the vehicles of AA and ENA (control group); ENA therapy (ENA group); AA alone (AA group); AA and ENA (AA+ENA group); and AA and ENA being started from day 10 (AA+ENAd10 group). As previously described [11], the salt depletion was achieved by administrating a single dose of furosemide (4 mg/kg body wt, intraperitoneally; Hoechst Marion Roussel, Frankfurt, Germany) one week before starting the protocol, and by maintaining animals on a low-sodium, normal-protein diet (0.05% sodium; Carfil Quality, Oud-Turnhout, Belgium) throughout the study.

In the second protocol (Table 1), weight-matched rats fed with a normal sodium diet (0.20%) were randomly assigned to four groups and received the following drugs for 35 days: the vehicles of AA and ENA+CSN (control group); ENA+CSN combined therapy (ENA+CSN group); AA alone (AA group); and AA and ENA+CSN combined therapy (AA+ENA+CSN group). To assess the effect of dietary sodium intake on AA-induced nephropathy, a fifth group was added and consisted of AA-treated rats after salt depletion conditioning, as described above. In a third longer-duration protocol (Table 1), rats intoxicated by AA for 35 days still received ENA+CSN until day 65 and were compared with AA-treated rats ($N = 6$).

At the end of each observation period, systolic blood pressure (sBP) was noninvasively measured with a modern electronic version of the sphygmomanometer method (AH 50–3046; Harvard Apparatus, Ltd., Edenbridge,

UK), and urine collection was performed by placing animals in metabolic cages. Afterwards, rats were deeply anesthetized with ketamine and xylazine, and blood samples were taken by intracardiac puncture with a syringe containing potassium-EDTA. Urine and blood samples were centrifugated at 1600*g* for 15 minutes at 4°C and stored at −20°C until assayed. Kidneys were quickly removed, decapsulated, and weighed. The right kidney was hemisected, rinsed in saline, and fixed in 4% buffered formaldehyde for morphologic studies for one part, and snap frozen for immunohistochemistry for the other part. The left kidney was rinsed, put in liquid nitrogen, and stored at −80°C for enzyme activity analyses.

Renal biochemical parameters

Plasma creatinine levels were determined by using a sensitive accurate high-performance liquid chromatography (HPLC) method, as previously described [25]. An automated analyzer (Modular Hitachi, Roche Diagnostics Division, Vilvoorde, Belgium) was used for the determination of urinary sodium. Urinary creatinine and protein levels were measured using the pseudokinetic Jaffé method (Creatinine Diagnostic Kit, Sigma-Aldrich, Bornem, Belgium) and the Bradford dye binding assay [26], respectively. Twenty micrograms of urinary protein contents were loaded per lane and were electrophoretically separated on a 12% sodium dodecyl sulfate-polyacrylamide gel (SDS-PAGE). The protein bands were revealed by staining with Coomassie blue dye in 50% methanol and 10% glacial acetic acid followed by destaining. In order to evaluate the proximal tubular brush border integrity, leucine aminopeptidase (LAP) activity was measured in urine using a spectrofluorometric assay after 1:30 and 1:60 dilution of the urine samples with 50 mmol/L Tris HCl buffer (pH 7.6) [25]. Results were expressed as μmol 7-amido-4-methyl coumarin (AMC) produced per mmol of urinary creatinine.

Measurement of renal angiotensin-converting enzyme activity

About 50 mg of renal tissue was homogenized in 2 mL of HEPES buffer (HEPES 50 mmol/L, $MgCl_2$ 10 mmol/L, Triton X-100 0.1%, pH 7.4) and centrifugated at 12,000*g* for 15 minutes at 4°C. ACE activity was measured in the supernatant by using a spectrophotometric method [27]. Ten microliters of supernatant was mixed with 120 μL of the substrate hippuryl-L-histidyl-L-leucine solution (Sigma-Aldrich, Bornem, Belgium) and incubated for 15 minutes at 37°C. Reaction was stopped by adding 725 μL NaOH 0.28 mol/L, and L-histidyl-L-leucine formed under the action of ACE was spectrofluorimetrically quantified after being complexed with 50 μL of O-phthaldialdehyde (excitation and emission wavelengths of 360 and 500 nm, respectively). ACE activity was expressed as μmol of L-histidyl-L-leucine produced per minute, and per milligram of protein.

Histopathologic study

For light microscopy, transversal paraffin-embedded sections (5 μm thick) of the kidney were prepared and stained with hematoxylin-eosin and Goldner's trichrome. Renal interstitial fibrosis was quantitated on Goldner's trichrome-stained sections by evaluating the interstitial matrix expansion with a point-counting technique [28, 29]. Sections of paraffin-embedded renal tissue were visualized on a computer display with an Olympus DP50 camera connected to a light Olympus BX51 microscope (Olympus Optical Co., Tokyo, Japan) at original magnification of ×200. Up to 20 separate, nonoverlapping microscopic fields of renal cortex from each rat were digitalized and saved on the hard disk of a personal computer. The fractional volume occupied by the interstitial fibrosis was evaluated by overlaying a 16 × 12-point grid on the recorded digital image and defined as the ratio of points lying within the fibrosis (stained in green) divided by the total number of points. Values were averaged to yield a mean score of each kidney (expressed as a percentage). Quantitation processes were made in a blinded and randomized fashion.

Immunohistochemical staining

Mouse monoclonal antibodies were used for the detection of α-smooth muscle actin (αSMA, Clone 1A4, dilution 1:100; Dako, Glostrup, Denmark) and proliferating cell nuclear antigen (PCNA, clone PC10, 1:100; Dako). For labeling of collagens I and IV, samples were incubated overnight with goat anti-type I collagen (1:20 dilution, SouthernBiotech, Birmingham, AL, USA) and anti-type IV collagen (1:40 dilution, SouthernBiotech). These immunostainings were performed on deparaffinized and dehydrated 4% paraformaldehyde-fixed sections.

Evaluation of monocyte/macrophage interstitial infiltration was done by using an immunohistochemical detection with mouse monoclonal antibodies recognizing the ED1 antigen (Serotec, Oxford, UK) on cryostat sections (8 μm thick) of frozen kidneys. Immunoperoxidase staining was performed using a commercial kit (ABC kit, Vector Laboratories, Inc., Burlingame, CA, USA). The endogenous peroxidase activity was blocked in 1% hydrogen peroxide in methanol solution. Slides were rinsed in TBS, and were incubated with 5% nonspecific horse serum (Vector Laboratories) for 10 minutes in order to prevent a cross-reaction of horse antimouse serum with rat IgG. The sections were then rinsed in TBS, incubated in avidin solution for 15 minutes, rinsed again in TBS, and incubated in biotin solution for 15 minutes in order to inactivate endogenous biotin. Sections were incubated

overnight at 4°C with the primary antibodies, then incubated with biotinylated horse antimouse or antigoat immunoglobulins (Vector Laboratories) according to the primary antibody, and finally incubated with avidin/biotin complex. The color development was performed with the chromogen 3,3′-diaminobenzidene, and sections were counterstained with hematoxylin. For negative controls, the same protocol was performed omitting the first antibody.

To quantify the degree of ED-1–positive cells infiltration, up to 20 cortical fields (×200) were digitalized using Olympus DP50 camera mounted on Olympus BX51 microscope (Olympus Optical Co., Tokyo, Japan). The ED-1 immunostaining was morphometrically measured by evaluating the labeling index with a computer-assisted image analyser system based on the NIH Image analysis software (Scion Image version b4.0.2; Scion Corporation, Frederick, MA, USA). The software enabled the operator to substract the background, and to set density threshold values corresponding to the staining. The labeling index was defined as the area above threshold divided by the frame area, and represented the percentage of the total examined area that positively stained. Quantification was performed blinded to the identity of the sections.

Statistical analyses

Results are expressed as mean ± SEM. Individual comparisons between two groups were performed with Student *t* test. Comparison between multiple groups was made using one-way analysis of variance (ANOVA) followed by Bonferroni's post-test. Nonparametric data were compared by using the Kruskal-Wallis test, followed by the Mann-Whitney rank test. Differences were considered significant if the P value was < 0.05.

RESULTS

Effect of ENA on blood pressure, renal ACE activity, and biochemical parameters in the salt-depleted rat model of AAN (protocol 1)

Thirty-five days of AA injections to salt-depleted rats produced an increase in renal ACE activity without affecting sBP (Table 2). Given to control rats, ENA significantly reduced sBP and renal ACE activity. In AA groups receiving ENA, renal ACE activity was also significantly inhibited, whereas sBP was decreased without reaching a significant statistical level (Table 2).

Renal function analyses performed on day 35 are listed in Table 3. There were no significant differences between control and ENA groups. Aristolochic acid-treated rats exhibited a significant increase in plasma creatinine and proteinuria, as well as a decrease in urinary LAP activity compared with controls. Whenever ENA was initiated (from day 10 or 0), no change in renal function impairment induced by AA was noticed.

Table 2. Effect of ACE inhibition on blood pressure and renal ACE activity in AA-treated rats fed with a low sodium diet on day 35 (protocol 1)

Rat groups	Systolic blood pressure *mm Hg*	Renal ACE activity *μmol His-Leu/min/g protein*
Control	115.5 ± 9.9	53.1 ± 21.6[a]
ENA	90.9 ± 5.3[b]	2.4 ± 2.4[b]
AA	126.4 ± 12.1	118.2 ± 32.2
AA + ENA	101.6 ± 9.6	4.6 ± 3.3[b,c]
AA + ENAd10	96.9 ± 5.7	4.0 ± 4.0[b,c]

Abbreviations are: ACE, angiotensin-converting enzyme; His-Leu, histidyl-leucine; ENA, enalapril (10 mg/kg body wt) started from day 0; AA, aristolochic acids (10 mg/kg body wt); ENAd10, enalapril (10 mg/kg body wt) started from day 10. Data are the mean ± SEM for seven rats/group, except for control group ($N = 6$).

[a] $N = 5$; one determination could not be performed.

[b] $P < 0.01$, compared with control rats.

[c] $P < 0.05$, compared with AA-treated rats.

Table 3. Effect of ACE inhibition on renal function in AA-treated rats fed with a low sodium diet on day 35 (protocol 1)

	Plasma creatinine *μmol/L*	Proteinuria *g/mmol creatinine*	Urinary LAP activity *μmol AMC/mmol creatinine*
Control	26.9 ± 1.8	0.11 ± 0.01	116.4 ± 4.8
ENA	33.3 ± 3.5	0.15 ± 0.02	100.6 ± 10.6
AA	63.9 ± 4.9[a]	0.35 ± 0.04[b]	17.6 ± 3.1[b]
AA + ENA	70.1 ± 8.1[c]	0.41 ± 0.05[b]	18.7 ± 1.3[b]
AA + ENAd10	80.9 ± 12.9[c]	0.44 ± 0.03[b]	26.9 ± 3.3[b]

Abbreviations are: LAP, leucine aminopeptidase; AMC, 7-amido-4-methyl coumarin; ENA, enalapril (10 mg/kg body wt) started from day 0; AA, aristolochic acids (10 mg/kg body wt); ENAd10, enalapril (10 mg/kg body wt) started from day 10. Data are the mean ± SEM for seven rats/group, except for control group ($N = 6$).

[a] $P < 0.05$, compared with control rats.

[b] $P < 0.001$, compared with control rats.

[c] $P < 0.01$, compared with control rats.

Effect of ENA on renal morphologic parameters in the salt-depleted rat model of AAN (protocol 1)

In the control and ENA groups, no significant abnormality was observed in the renal tissue samples obtained on day 35. On the contrary, numerous foci of tubular atrophy and mononuclear cells infiltration, surrounded by severe interstitial fibrosis, were found in the deep cortex, the outer medulla, and the medullary rays from AA-treated rats. The injured tubules showed a sustained regenerative process, as reflected by an increase of PCNA-positive proximal tubule cells (Fig. 1A and B). The tubulointerstitial lesions were also characterized by the presence of α-SMA–positive myofibroblasts and the enlargement of interstitium due to collagen type IV deposition (Fig. 1C to F). As depicted in Figure 2A, the fractional volume of interstitial fibrosis was dramatically increased in the AA group. The treatment with ENA did not result in any change of this AA-induced renal fibrosis.

Around the injured tubules, the renal interstitium was infiltrated by ED-1 + monocytes/macrophages after 35 days of AA injections. When given from day 10 to AA-treated rats, ENA induced a 35% reduction of

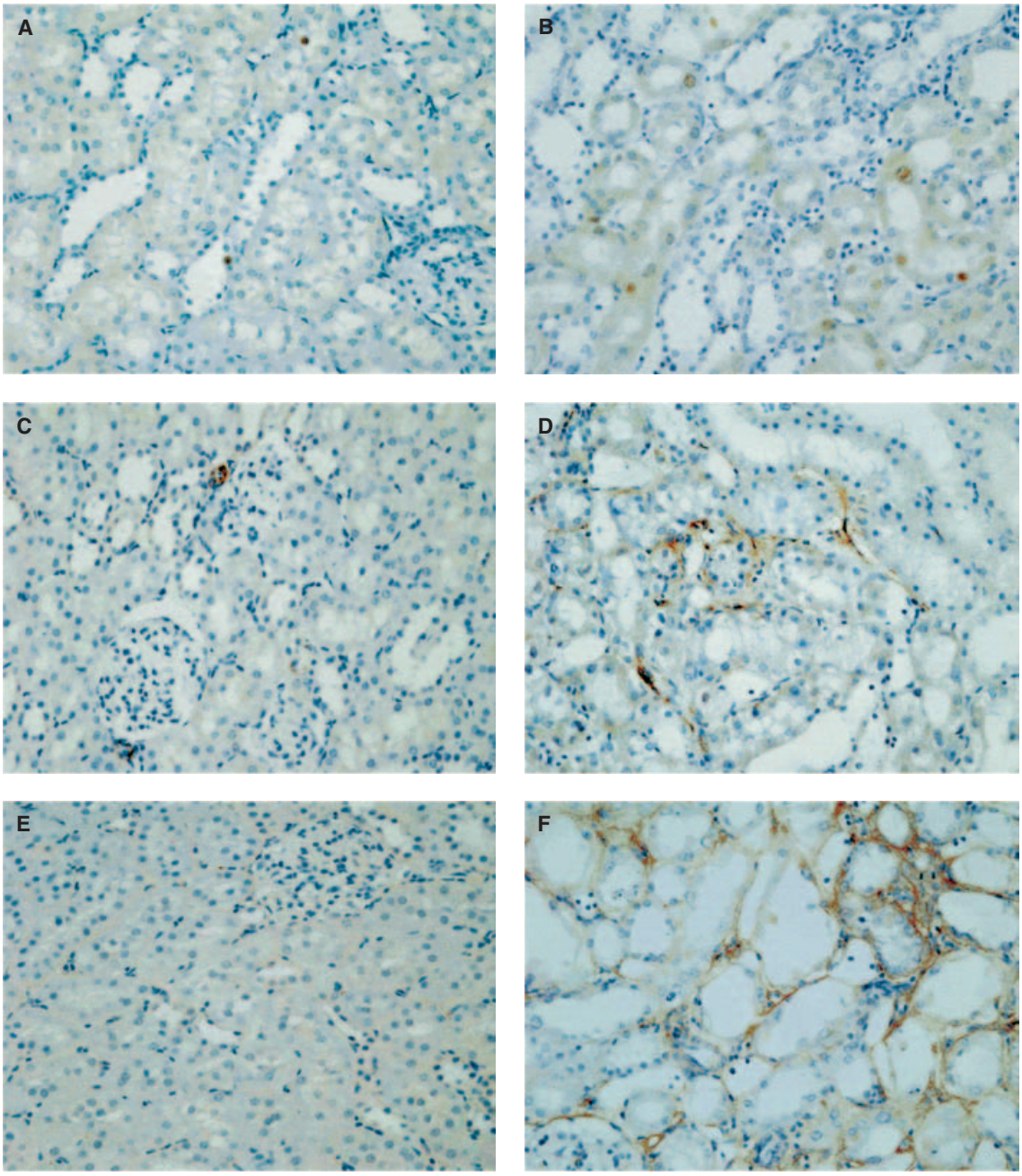

Fig. 1. Light microscopy of immunostaining for proliferating cells (*A*, *B*), α-smooth muscle actin–positive myofibroblasts (*C*, *D*), and collagen type IV (*E*, *F*). Photomicrographs (×400) of renal cortex from representative salt-depleted rats (protocol 1) receiving vehicle (A, C, E) and aristolochic acids (B, D, F). Rats treated with aristolochic acids for 35 days showed foci of tubulointerstitial injuries characterized by regenerative PCNA-positive tubular cells (B), the presence of α-SMA–positive myofibroblasts (D), and the enlargement of interstitium due to collagen type IV deposition (F).

macrophages infiltration. This reduction exceeded 50% when ENA was administrated as early as day 0 (Fig. 2B).

Effect of the salt diet on the development of the rat model of AAN (protocol 2)

As shown in Table 4 comparing AA-treated rats fed with a normal sodium diet to those fed with a low sodium diet, the urinary sodium excretion was significantly decreased in animals kept on low sodium diet. However, no statistical difference was found between the two groups in terms of sBP, renal ACE activity, plasma creatinine, proteinuria, fractional volume of interstitial fibrosis, and ED-1 positive cells infiltration. Histologic tubulointerstitial injuries consisting in tubular atrophy and regeneration, inflammatory and myofibroblast cell infiltration, interstitial fibrosis, and collagen type IV deposition were found in AA-treated rats, irrespective of the dietary sodium intake.

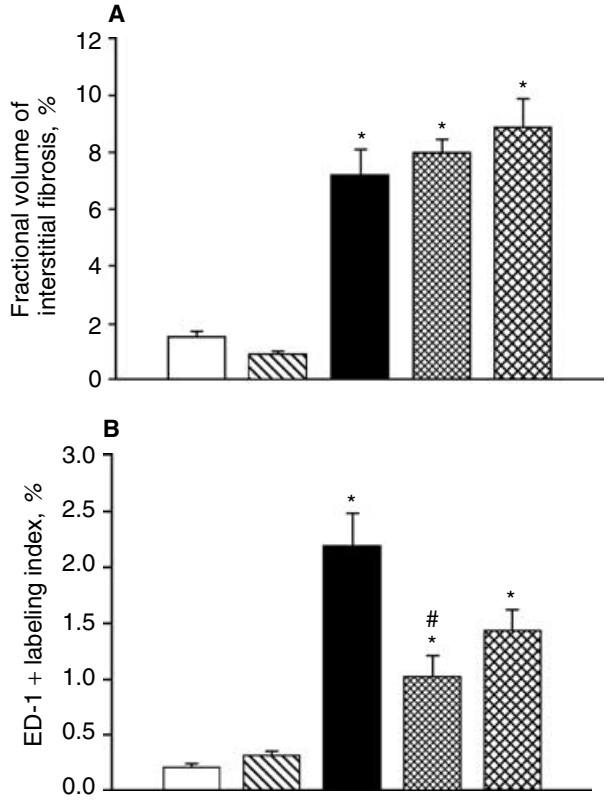

Fig. 2. Semiquantitative evaluation of the fractional volume occupied by interstitial fibrosis (*A*) and ED-1 + monocytes/macrophages infiltration (*B*) in the renal cortex (protocol 1). Values are expressed as mean ± SEM from sodium-depleted rats given vehicle (control, $N = 6$), enalapril (ENA, $N = 7$), aristolochic acids (AA, $N = 7$), aristolochic acids + enalapril started from day 0 (AA+ENA, $N = 7$), and aristolochic acids + enalapril started from day 10 (AA+ENAd10, $N = 7$). Symbols are: □, control; ▨, ENA; ■, AA; ▩, AA + ENA; ▩, AA + ENAd10. $^{*}P < 0.01$ vs. control and $^{\#}P < 0.01$ vs. AA.

Effect of the combined therapy (ENA+CSN) on blood pressure, renal ACE activity, and biochemical parameters in rats receiving a normal sodium diet and AA (protocol 2)

Despite a significant increase in renal ACE activity, no significant change in sBP was observed in rats treated by AA when compared to controls (Table 5). By contrast, AA-intoxicated animals given the combined therapy ENA+CSN showed a reduced sBP and an inhibition of renal ACE activity (Table 5). However, this inhibition did not result in any change in renal functional parameters such as plasma creatinine, proteinuria and urinary LAP activity (Table 6). Of note, the electrophoretic patterns of proteinuria observed in AA-treated rats consisted in albuminuria and low-molecular-weight proteins. These patterns were similar to those found in control rats, as well as in animals treated with the combined therapy ENA + CSN (data not shown).

Table 4. Effect of dietary sodium intake on the development of the rat model of AA nephropathy on day 35 (protocol 2)

	AA—normal sodium diet $N = 6$	AA—low sodium diet $N = 7$
uNa/uCr	28.7 ± 2.2	5.5 ± 1.4[a]
sBP	148.6 ± 5.6	149.0 ± 5.6
Renal ACEa	167.8 ± 40.1	215.9 ± 69.1
pCr	40.4 ± 10.4	30.1 ± 5.5
uPr	0.33 ± 0.02	0.32 ± 0.04
Interstial fibrosis %	5.6 ± 0.4	6.8 ± 1.1
ED-1 + cells %	5.8 ± 1.0	3.9 ± 0.7

Abbreviations are: AA, aristolochic acids (10 mg/kg body wt); uNa/uCr, urinary sodium excretion (mmol/mmol creatinine); sBP, systolic blood pressure (mm Hg); ACEa, angiotensin-converting enzyme activity (μmol histidyl-leucine produced/min/g protein); pCr, plasma creatinine (μmol/L); uPr, proteinuria (g/mmol creatinine); ED-1 +, monocytes/macrophages. Data are the mean ± SEM.

[a] $P < 0.0001$ compared with AA—normal sodium diet group.

Table 5. Effect of combined therapy (ENA + CSN) on blood pressure and renal ACE activity in AA-treated rats fed with a normal sodium diet on day 35 (protocol 2)

Rat groups	Systolic blood pressure *mm Hg*	Renal ACE activity *μmol His-Leu/min/g protein*
Control	140.1 ± 8.2	85.6 ± 10.8
ENA + CSN	110.6 ± 2.0[a]	3.16 ± 3.16[b]
AA	148.6 ± 9.2	167.8 ± 40.1[c]
AA + ENA + CSN	106.0 ± 3.9[a,d]	31.9 ± 17.8[c,e]

Abbreviations are: ACE, angiotensin-converting enzyme; His-Leu, histidyl-leucine; ENA, enalapril (10 mg/kg body wt); CSN, candesartan cilexetil (7 mg/kg body wt); AA, aristolochic acids (10 mg/kg body wt). Data are the mean ± SEM for seven rats/group, except for AA group ($N = 6$).

[a] $P < 0.01$, compared with control rats.
[b] $P < 0.001$, compared with control rats.
[c] $P < 0.05$, compared with control rats.
[d] $P < 0.001$, compared with AA-treated rats.
[e] $P < 0.01$, compared with AA-treated rats.

Table 6. Effects of combined therapy (ENA + CSN) on renal function in AA-treated rats fed with a normal sodium diet on day 35 (protocol 2)

Rat groups	Plasma creatinine *μmol/L*	Proteinuria *g/mmol creatinine*	Urinary LAP activity *μmol AMC/mmol creatinine*
Control	15.9 ± 0.8	0.15 ± 0.01	45.7 ± 8.1
ENA + CSN	16.2 ± 0.9	0.13 ± 0.01	65.7 ± 18.5
AA	40.4 ± 10.4[a]	0.33 ± 0.02[b]	9.8 ± 2.6[c]
AA + ENA + CSN	37.4 ± 9.4[c]	0.30 ± 0.02[b]	10.0 ± 0.9[b]

Abbreviations are: LAP, leucine aminopeptidase; AMC, 7-amido-4-methyl coumarin; ENA, enalapril (10 mg/kg body wt); CSN, candesartan cilexetil (7 mg/kg body wt); AA, aristolochic acids (10 mg/kg body wt). Data are the mean ± SEM for seven rats/group, except for AA group ($N = 6$).

[a] $P < 0.05$, compared with control rats.
[b] $P < 0.001$, compared with control rats.
[c] $P < 0.01$, compared with control rats.

Effect of the combined therapy (ENA+CSN) on renal morphologic parameters in rats receiving a normal sodium diet and AA (protocol 2)

No renal histopathologic change was found in the control and ENA+CSN groups. Typical morphologic findings of AA-induced nephropathy consisting in tubular

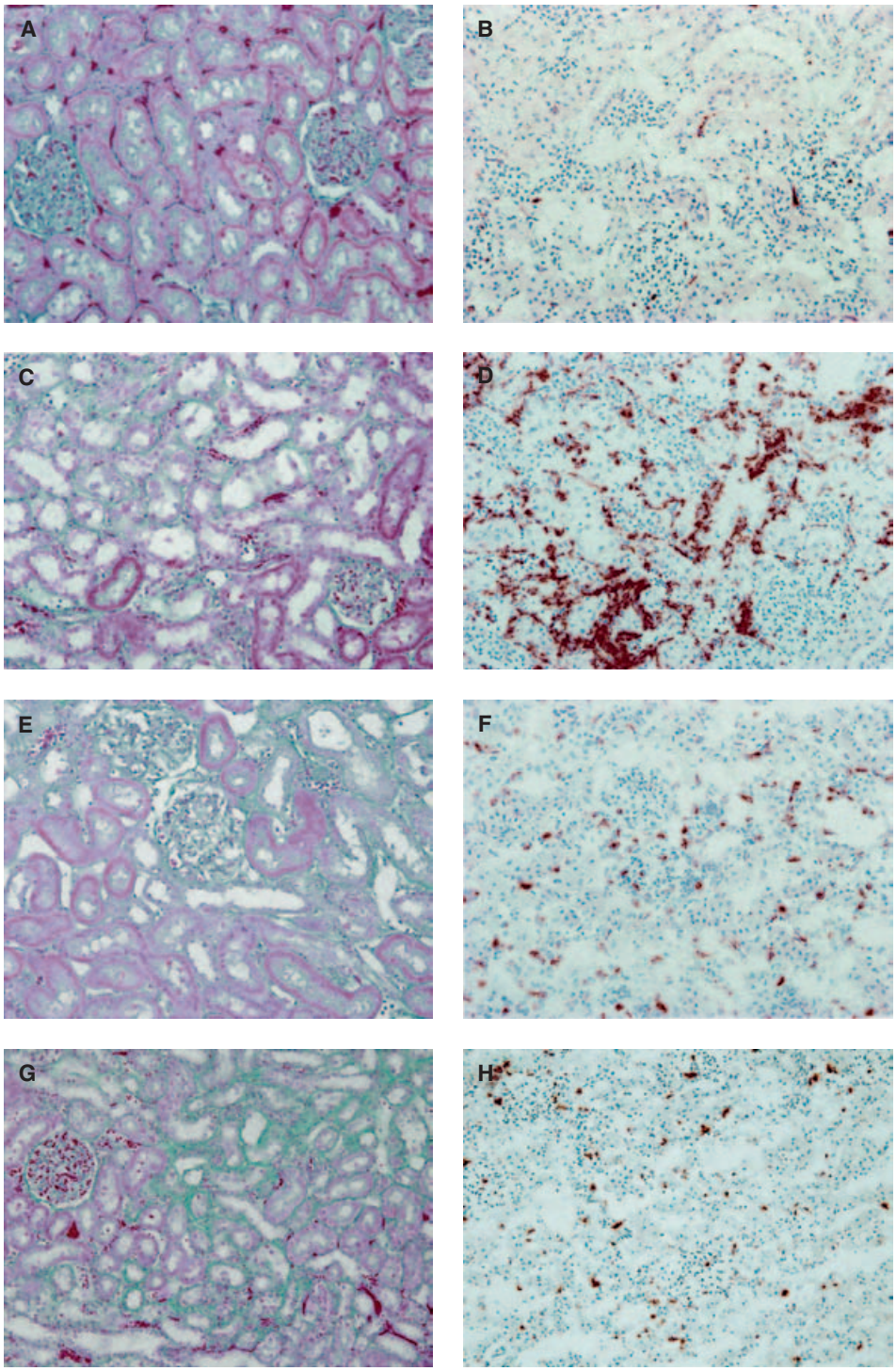

Fig. 3. Light microscopy of Goldner's trichrome-stained sections (*A*, *C*, *E*, *G*) and immunostaining for ED1 + monocytes/macrophages (*B*, *D*, *F*, *H*). Photomicrographs (×200) of renal cortex on day 35 from representative rats (protocol 2) given vehicle (A, B), aristolochic acids (C, D), and aristolochic acids combined with enalapril plus candesartan (E, F), and on day 65 from representative rats (protocol 3) receiving AA for 35 days and enalapril plus candesartan for 65 days (G, H).

atrophy, mononuclear cells infiltrate, and interstitial fibrosis (Fig. 3A to F) were observed in both AA and AA+ENA+CSN groups. PCNA-postive proliferating tubule cells, α-SMA myofibroblasts, and collagen type IV deposition were also found. The ED-1 immunostaining confirmed the accumulation of macrophages into the renal interstitium from AA-treated rats compared with control rats.

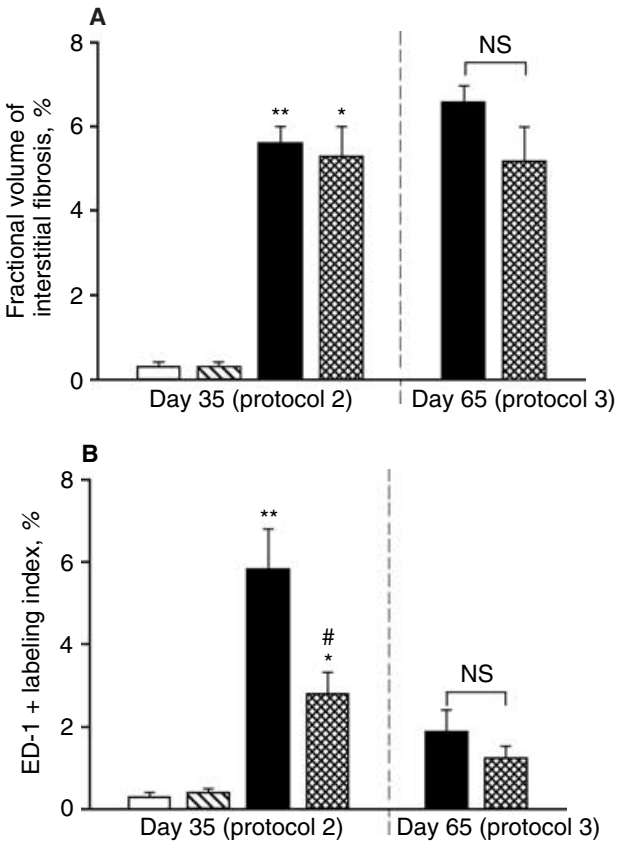

Fig. 4. Semiquantitative evaluation of the fractional volume of interstitial fibrosis (*A*) and ED-1 + monocytes/macrophages infiltration (*B*) in the renal cortex. In the protocol 2, values are expressed as mean ± SEM from rats fed with a normal sodium diet and given vehicle (control, $N = 7$), enalapril combined with candesartan (ENA + CSN, $N = 7$), aristolochic acids (AA, $N = 6$), and aristolochic acids treated with enalapril plus candesartan (AA+ENA+CSN, $N = 7$) for 35 days. In the protocol 3, values are expressed as mean ± SEM from rats fed with a normal sodium diet and given aristolochic acids for 35 days (AA, $N = 6$) alone or with enalapril plus candesartan for 65 days (AA+ENA+CSN, $N = 4$). Symbols are: □, control; ▨, ENA + CSN; ■, AA; ▩, AA + ENA + CSN. $^{*}P < 0.001$ vs. control; $^{**}P < 0.01$ vs. control and $^{\#}P < 0.01$ vs. AA.

The fractional volume of interstitial fibrosis was markedly increased to a similar extent in both AA groups, untreated or treated with ENA+CSN (Fig. 4A). By contrast, this combined therapy administrated to AA-treated rats induced a twofold decrease of monocyte/macrophage infiltration (Fig. 4B).

Effect of the combined therapy (ENA+CSN) given for up to 65 days on blood pressure, renal biochemical, and morphologic parameters in rats receiving a normal sodium diet and AA (protocol 3)

In the group of AA-intoxicated rats treated with ENA + CSN, two rats were found dead (one at day 18 due to accidental water deprivation, and one at day 64 due to severe hypotension). Typical tubulointerstitial injuries as described above were observed in both AA-intoxicated rat groups, given (Fig. 3G and H) or not given the ENA + CSN therapy. When ENA + CSN were administrated to AA-intoxicated rats, sBP was decreased on day 65, but biochemical (Table 7) and morphologic (Fig. 4) alterations induced by AA were unchanged.

Table 7. Effect of the combined therapy (ENA+CSN) on blood pressure, renal biochemical, and morphologic parameters in rats receiving a normal sodium diet and AA on day 65 (protocol 3)

	AA for 35 days	AA for 35 days + ENA + CSN for 65 days
sBP	133.7 ± 5.7	91.2 ± 3.9[a]
pCr	25.7 ± 1.1	25.2 ± 1.6
uPr	0.17 ± 0.01	0.14 ± 0.04
uLAP	13.6 ± 1.3	8.9 ± 2.0

Abbreviations are: AA, aristolochic acids (10 mg/kg body wt); ENA, enalapril (10 mg/kg body wt); CSN, candesartan cilexetil (7 mg/kg body wt); sBP, systolic blood pressure (mm Hg); pCr, plasma creatinine (μmol/L); uPr, proteinuria (g/mmol creatinine); uLAP, urinary leucine aminopeptidase activity (μmol 7-amido-4-methyl coumarin produced/mmol creatinine). Data are the mean ± SEM for six rats/group, except for AA + ENA + CSN group, in which two rats were found dead.

[a] $P < 0.001$.

DISCUSSION

In the past decade, a new type of rapidly progressive interstitial fibrosis has been reported after exposure to nephrotoxic aristolochic acids contained in plants of *Aristolochia* species (reviewed in [9]). Recently, a reproducible short-term model of chronic AAN was developed in salt-depleted male Wistar rats [11, 25]. As demonstrated for the cyclosporine A–induced nephropathy rat model [12], stimulation of the intrarenal RAS via sodium depletion seemed to be prerequired to enhance the renal interstitial fibrosis process. In the present study, we demonstrated that similar tubulointerstitial insults could be obtained in AA-treated rats fed a normal sodium diet compared to a salt-depletion conditioning. Moreover, the RAS blockade with ACE inhibitor ± AT1RA concomitant to AA-injections for 35 days significantly reduced the macrophages infiltration, but had no beneficial effect on the renal functional impairment or interstitial fibrosis. The dual RAS blockade therapy given for an extended period of 65 days also failed to prevent AA-induced nephropathy in this model.

Our initial model of AAN was designed on the basis of the cyclosprine A–induced nephropathy rat model, suggesting that RAS stimulation was important in the induction of tubulointerstitial lesions [11]. Interestingly, the renal ACE activity was not enhanced by the salt restriction. These data are consistent with recent experimental results showing that salt depletion in rats increased the renin activity and angiotensin I and II production without affecting ACE activity [30]. By contrast, the renal ACE activity was increased in rats intoxicated by AA with the same extent in both dietary sodium conditions. Although intrarenal Ang II levels were not directly

measured, we can consider that elevated ACE activity reflected a stimulation of the local RAS and an enhancement of Ang II generation. This activation of the intrarenal RAS could derive from two main origins. First, in response to renal injurious stimuli, proximal tubule cells may express mRNA for renin, angiotensinogen, and ACE [31]. Second, several studies have shown that monocytes/macrophages can express all the components of the RAS and produce Ang II [32]. Since Ang II was demonstrated to be a chemotactic factor [33, 34], the activated inflammatory cells may contribute in turn to the progression and perpetuation of inflammation.

In the present rat model of AAN, the sodium depletion conditioning did not exacerbate the activation of intrarenal ACE activity or the severity of monocytes/macrophages interstitial infiltration. In parallel, similar tubulointerstitial injuries and renal impairment were found in AA-treated rats, irrespective of the dietary sodium intake. The tubular lesions, resulting from an imbalance between death and regenerating cells, were located in the deep cortex and the outer stripe of outer medulla with extension along the medullary rays, confirming that the pars recta of proximal tubule was the main target of AA-related nephrotoxicity [35, 36]. Foci of injured tubules were surrounded by infiltrating monocytes/macrophages and α-SMA myofibroblasts, as well as interstitial fibrosis characterized by collagen type IV deposition. Growing evidence suggests that α-SMA myofibroblasts, the main cells involved in the accumulation of interstitial extracellular matrix, are derived from tubular epithelium under pathologic conditions by a process of epithelial to mesenchymal transition [37, 38]. It is interesting to note that glomerular structures, as well as afferent and efferent arterioles, were not affected by AA-induced nephrotoxicity. These histologic findings were quite similar to those observed in patients suffering from the so-called Chinese herbs nephropathy (CHN) [4]. In renal tissue samples from CHN patients, the interstitial fibrosis was more extensive than in this rat model, with major loss of tubules and variable degree of inflammatory infiltrates. The glomeruli were relatively spared, whereas interlobular and afferent arterioles showed thickening of their walls. These differences in the severity of the histologic lesions actually reflect a more advanced stage of the disease in CHN patients.

Since intrarenal ACE activity was demonstrated to be enhanced, we hypothesized that ACE inhibitor, combined or not with AT1RA, could exhibit renoprotective effects. It has been largely demonstrated that RAS blockade attenuated the glomerulosclerosis and tubulointerstitial fibrosis jointly to reduce proteinuria and glomerular filtration rate (GFR) decline in a broad range of experimental renal diseases models, such as anti-Thy1 mesangial proliferative glomerulonephritis [39], chronic aminonucleoside nephrosis [40], passive Heymann nephritis [41], diabetic nephropathy [42], renal mass reduction [43], obstructive nephropathy [44], and cyclosporine nephropathy [45]. Nevertheless, in the present rat model of chronic interstitial fibrosis, RAS blockade by either an ACE inhibitor alone or combined with an AT1RA did not prevent the renal function impairment induced by AA. One possible explanation could be insufficient doses of ACE inhibitor or AT1RA given to AA-intoxicated rats. However, RAS seemed to be correctly blocked at the dose of 10 mg/kg body wt of ENA and 7 mg/kg body wt of CSN, as attested by a sustained decrease of sBP and an almost complete inhibition of renal ACE activity. Another explanation for the lack of positive effect on plasma creatinine could be the fall of sBP due to RAS blockade, resulting in reduced renal perfusion and a decrease of GFR. Interestingly, similar observations were also reported in the cyclosporine A–induced nephropathy treated with ENA or losartan or a combination of these drugs [45].

Nephroprotective effects of RAS blockade are largely attributed to its ability to reduce proteinuria and, in particular, albuminuria. Indeed, proteins filtered in excessive quantities and reabsorbed by proximal tubule cells cause injury by lysosome rupture, and induce phenotypic changes, which in turn lead to interstitial inflammatory reaction and fibrosis [46]. Rats intoxicated with AA developed after 35 days a moderate proteinuria with an electrophoretic pattern mainly comparable to this observed in control rats. It is reasonable to think that AA-induced proteinuria was the consequence of proximal tubular damage, rather than glomerular barrier alteration, which might explain the absence of effects of RAS blockade on this proteinuria.

A striking finding of our study was the severe interstitial accumulation of monocytes/macrophages induced by AA. These mononuclear cells, found in most of progressive renal diseases irrespectively of their underlying cause, are considered to be an important source of fibrosis-promoting growth factors, vasoactive molecules, and even matrix proteins [47, 48]. In several models of renal injury, RAS blockade results in a reduction of macrophage infiltration and fibrosis [49–51]. Similarly, in the present rat model of AAN, a significant reduction of monocytes/macrophages infiltration was observed following ENA or ENA plus CSN administration to AA-treated rats. However, ED-1 staining does not distinguish activated macrophages from inactive monocytes, and thus, the contribution of mononuclear cells infiltration in the pathogenesis of AAN is largely unknown and remains to be investigated. Despite this putative beneficial effect of the RAS blockade, renal interstitial fibrosis and chronic renal failure were not prevented on day 35, as well as on day 65. One may object that renal fibrosis was evaluated by a semiquantitative scoring system, which could not be able to detect some slight changes. Anyway,

renal failure was obviously unaffected by RAS blockade, as reflected by similar elevated plasma creatinine in AA groups given or not the therapy.

CONCLUSION

The absence of enhancing effect of RAS stimulation on AAN allows us to simplify the protocol design for further experiments by omiting the salt-depletion procedure. On the other hand, the RAS blockade with an ACE inhibitor alone or combined with an AT1RA does not improve renal functional parameters and tubulointerstitial fibrosis in this rat model of AAN, despite a significant decrease in the monocytes/macrophages infiltration. Our data suggest that some pathways from renal injury to progressive fibrosis may be RAS independent.

ACKNOWLEDGMENTS

Dr. Debelle is a research fellow of Université Libre de Bruxelles (Brussels, Belgium). The authors are very grateful to Ms. Catherine Lebeau for her excellent technical assistance. This work was supported by grants from the Groupement pour l'Etude, le Traitement et la Réhabilitation Sociale des Insuffisants Rénaux Chroniques, the Fonds de la Recherche Scientifique Médicale (Belgium), and the Fondation Erasme (Hôpital Erasme, Brussels, Belgium). Parts of this work were presented at the 35th Congress of the American Society of Nephrology, Philadelphia, Pennsylvania, October 30 to November 4, 2002, and at the Annual Scientific Meeting of the Belgian Society of Nephrology, Antwerpen, Belgium, May 22, 2003.

Reprint requests to Frédéric Debelle, M.D., Department of Nephrology, Erasme Hospital, Route de Lennik, 808, B-1070 Brussels, Belgium. E-mail: fdebelle@ulb.ac.be

REFERENCES

1. Risdon RA, Sloper JC, De Wardener HE: Relationship between renal function and histological changes found in renal-biopsy specimens from patients with persistent glomerular nephritis. *Lancet* 2:363–366, 1968
2. Schainuck LI, Striker GE, Cutler RE, Benditt EP: Structural-functional correlations in renal disease. II. The correlations. *Hum Pathol* 1:631–641, 1970
3. Vanherweghem JL, Depierreux M, Tielemans C, *et al*: Rapidly progressive interstitial renal fibrosis in young women: Association with slimming regimen including Chinese herbs. *Lancet* 341:387–391, 1993
4. Depierreux M, Van Damme B, Vanden Houte K, Vanherweghem JL: Pathologic aspects of a newly described nephropathy related to the prolonged use of Chinese herbs. *Am J Kidney Dis* 24:172–180, 1994
5. Vanhaelen M, Vanhaelen-Fastre R, But P, Vanherweghem JL: Identification of aristolochic acid in Chinese herbs. *Lancet* 343:174, 1994
6. Cosyns JP, Jadoul M, Squifflet JP, *et al*: Chinese herbs nephropathy: A clue to Balkan endemic nephropathy? *Kidney Int* 45:1680–1688, 1994
7. Cosyns JP, Jadoul M, Squifflet JP, *et al*: Urothelial lesions in Chinese-herb nephropathy. *Am J Kidney Dis* 33:1011–1017, 1999
8. Nortier JL, Martinez MC, Schmeiser HH, *et al*: Urothelial carcinoma associated with the use of a Chinese herb (*Aristolochia fangchi*). *N Engl J Med* 342:1686–1692, 2000
9. Vanherweghem JL, Debelle FD, Muniz-Martinez MC, Nortier J: Aristolochic acid nephropathy after Chinese herbal remedies, in *Clinical Nephrotoxins*, 2nd ed, edited by De Broe ME, Porter GA, Bennett WM, Verpooten GA, Dordrecht, Kluwer Academic Publishers, 2003, pp 579–586
10. Cosyns JP, Goebbels RM, Liberton V, *et al*: Chinese herbs nephropathy-associated slimming regimen induces tumours in the forestomach but no interstitial nephropathy in rats. *Arch Toxicol* 72:738–743, 1998
11. Debelle FD, Nortier JL, de Prez EG, *et al*: Aristolochic acids induce chronic renal failure with interstitial fibrosis in salt-depleted rats. *J Am Soc Nephrol* 13:431–436, 2002
12. Young BA, Burdmann EA, Johnson RJ, *et al*: Cyclosporine A induced arteriolopathy in a rat model of chronic cyclosporine nephropathy. *Kidney Int* 48:431–438, 1995
13. Lewis EJ, Hunsicker LG, Bain RP, Rohde RD: The effect of angiotensin-converting-enzyme inhibition on diabetic nephropathy. The Collaborative Study Group. *N Engl J Med* 329:1456–1462, 1993
14. Ravid M, Savin H, Jutrin I, *et al*: Long-term stabilizing effect of angiotensin-converting enzyme inhibition on plasma creatinine and on proteinuria in normotensive type II diabetic patients. *Ann Intern Med* 118:577–581, 1993
15. Randomised placebo-controlled trial of effect of ramipril on decline in glomerular filtration rate and risk of terminal renal failure in proteinuric, non-diabetic nephropathy. The GISEN Group (Gruppo Italiano di Studi Epidemiologici in Nefrologia). *Lancet* 349:1857–1863, 1997
16. Ruggenenti P, Perna A, Gherardi G, *et al*: Renal function and requirement for dialysis in chronic nephropathy patients on long-term ramipril: REIN follow-up trial. Gruppo Italiano di Studi Epidemiologici in Nefrologia (GISEN). Ramipril Efficacy in Nephropathy. *Lancet* 352:1252–1256, 1998
17. Andersen S, Tarnow L, Rossing P, *et al*: Renoprotective effects of angiotensin II receptor blockade in type 1 diabetic patients with diabetic nephropathy. *Kidney Int* 57:601–606, 2000
18. Lewis EJ, Hunsicker LG, Clarke WR, *et al*: Renoprotective effect of the angiotensin-receptor antagonist irbesartan in patients with nephropathy due to type 2 diabetes. *N Engl J Med* 345:851–860, 2001
19. Campbell R, Sangalli F, Perticucci E, *et al*: Effects of combined ACE inhibitor and angiotensin II antagonist treatment in human chronic nephropathies. *Kidney Int* 63:1094–1103, 2003
20. Lafayette RA, Mayer G, Park SK, Meyer TW: Angiotensin II receptor blockade limits glomerular injury in rats with reduced renal mass. *J Clin Invest* 90:766–771, 1992
21. Zatz R, Dunn BR, Meyer TW, *et al*: Prevention of diabetic glomerulopathy by pharmacological amelioration of glomerular capillary hypertension. *J Clin Invest* 77:1925–1930, 1986
22. Kohzuki M, Yasujima M, Kanazawa M, *et al*: Antihypertensive and renal-protective effects of losartan in streptozotocin diabetic rats. *J Hypertens* 13:97–103, 1995
23. Imamura A, MacKenzie HS, Lacy ER, *et al*: Effects of chronic treatment with angiotensin converting enzyme inhibitor or an angiotensin receptor antagonist in two-kidney, one-clip hypertensive rats. *Kidney Int* 47:1394–1402, 1995
24. Klahr S, Ishidoya S, Morrissey J: Role of angiotensin II in the tubulointerstitial fibrosis of obstructive nephropathy. *Am J Kidney Dis* 26:141–146, 1995
25. Debelle F, Nortier J, Arlt VM, *et al*: Effects of dexfenfluramine on aristolochic acid nephrotoxicity in a rat model for Chinese-herb nephropathy. *Arch Toxicol* 77:218–226, 2003
26. Bradford MM: A rapid and sensitive method for the quantitation of microgram quantities of protein utilizing the principle of protein-dye binding. *Anal Biochem* 72:248–254, 1976
27. Friedland J, Silverstein E: A sensitive fluorimetric assay for serum angiotensin-converting enzyme. *Am J Clin Pathol* 66:416–424, 1976
28. Morrissey J, Hruska K, Guo G, *et al*: Bone morphogenetic protein-7 improves renal fibrosis and accelerates the return of renal function. *J Am Soc Nephrol* 13(Suppl 1):S14–S21, 2002
29. Guo G, Morrissey J, McCracken R, *et al*: Contributions of angiotensin II and tumor necrosis factor-alpha to the development of renal fibrosis. *Am J Physiol Renal Physiol* 280:F777–F785, 2001
30. Ingert C, Grima M, Coquard C, *et al*: Effects of dietary salt changes on renal renin-angiotensin system in rats. *Am J Physiol Renal Physiol* 283:F995–1002, 2002

31. Harris RC, Cheng HF: The intrarenal renin-angiotensin system: A paracrine system for the local control of renal function separate from the systemic axis. *Exp Nephrol* 4(Suppl 1):2–7, 1996
32. Okamura A, Rakugi H, Ohishi M, *et al*: Upregulation of renin-angiotensin system during differentiation of monocytes to macrophages. *J Hypertens* 17:537–545, 1999
33. Ruiz-Ortega M, Lorenzo O, Ruperez M, Egido J: ACE inhibitors and AT(1) receptor antagonists-beyond the haemodynamic effect. *Nephrol Dial Transplant* 15:561–565, 2000
34. Ruiz-Ortega M, Lorenzo O, Suzuki Y, *et al*: Proinflammatory actions of angiotensins. *Curr Opin Nephrol Hypertens* 10:321–329, 2001
35. Nortier JL, Deschodt-Lanckman MM, Simon S, *et al*: Proximal tubular injury in Chinese herbs nephropathy: Monitoring by neutral endopeptidase enzymuria. *Kidney Int* 51:288–293, 1997
36. Cosyns JP, Dehoux JP, Guiot Y, *et al*: Chronic aristolochic acid toxicity in rabbits: A model of Chinese herbs nephropathy? *Kidney Int* 59:2164–2173, 2001
37. Liu Y: Epithelial to mesenchymal transition in renal fibrogenesis: Pathologic significance, molecular mechanism, and therapeutic intervention. *J Am Soc Nephrol* 15:1–12, 2004
38. Lan HY: Tubular epithelial-myofibroblast transdifferentiation mechanisms in proximal tubule cells. *Curr Opin Nephrol Hypertens* 12:25–29, 2003
39. Peters H, Border WA, Noble NA: Targeting TGF-beta overexpression in renal disease: Maximizing the antifibrotic action of angiotensin II blockade. *Kidney Int* 54:1570–1580, 1998
40. Diamond JR, Anderson S: Irreversible tubulointerstitial damage associated with chronic aminonucleoside nephrosis. Amelioration by angiotensin I converting enzyme inhibition. *Am J Pathol* 137:1323–1332, 1990
41. Zoja C, Corna D, Camozzi D, *et al*: How to fully protect the kidney in a severe model of progressive nephropathy: A multidrug approach. *J Am Soc Nephrol* 13:2898–2908, 2002
42. Kato S, Luyckx VA, Ots M, *et al*: Renin-angiotensin blockade lowers MCP-1 expression in diabetic rats. *Kidney Int* 56:1037–1048, 1999
43. Taal MW, Chertow GM, Rennke HG, *et al*: Mechanisms underlying renoprotection during renin-angiotensin system blockade. *Am J Physiol Renal Physiol* 280:F343–F355, 2001
44. Ishidoya S, Morrissey J, McCracken R, Klahr S: Delayed treatment with enalapril halts tubulointerstitial fibrosis in rats with obstructive nephropathy. *Kidney Int* 49:1110–1119, 1996
45. Burdmann EA, Andoh TF, Nast CC, *et al*: Prevention of experimental cyclosporin-induced interstitial fibrosis by losartan and enalapril. *Am J Physiol* 269:F491–F499, 1995
46. Remuzzi G, Bertani T: Pathophysiology of progressive nephropathies. *N Engl J Med* 339:1448–1456, 1998
47. Nathan CF: Secretory products of macrophages. *J Clin Invest* 79:319–326, 1987
48. Nikolic-Paterson DJ, Lan HY, Hill PA, Atkins RC: Macrophages in renal injury. *Kidney Int* 45(Suppl):S79–S82, 1994
49. Ishidoya S, Morrissey J, McCracken R, *et al*: Angiotensin II receptor antagonist ameliorates renal tubulointerstitial fibrosis caused by unilateral ureteral obstruction. *Kidney Int* 47:1285–1294, 1995
50. Wu LL, Yang N, Roe CJ, *et al*: Macrophage and myofibroblast proliferation in remnant kidney: Role of angiotensin II. *Kidney Int* 63(Suppl):S221–S225, 1997
51. Ruiz-Ortega M, Bustos C, Hernandez-Presa MA, *et al*: Angiotensin II participates in mononuclear cell recruitment in experimental immune complex nephritis through nuclear factor-kappa B activation and monocyte chemoattractant protein-1 synthesis. *J Immunol* 161:430–439, 1998